Plasma enhanced chemical vapor deposition (PECVD) of SiOx thin films on Portuguese limestone: An experimental study

Journal of Cultural Heritage 70 (2024) 281–292

Contents lists available at ScienceDirect

Journal of Cultural Heritage

journal homepage: www.elsevier.com/locate/culher

VSI: In honour of Prof. Colombini

Plasma enhanced chemical vapor deposition (PECVD) of SiO_x thin films on Portuguese limestone: An experimental study

Yufan Ding[a,c], Sabrina Grassini[b], Emma Angelini[b], Nick Schiavon[a,*]

[a] Hercules Laboratory, University of Évora, Évora, Portugal
[b] Department of Applied Science and Technology, Polytechnic of Turin, Torino, Italy
[c] Centre for Archaeological Science, Sichuan University, China

ARTICLE INFO

Article history:
Received 16 August 2023
Accepted 2 October 2024

Keywords:
Batalha monastery
Oolitic limestone
Stone conservation
SiO_x coating
PECVD

ABSTRACT

Plasma Enhanced Chemical Vapor Deposition (PECVD) of SiO_x thin films has been applied to the stone surface under laboratory conditions in order to assess its feasibility as an alternative method for stone protection. SiO_x thin layers were deposited on oolitic limestone lithologies known to have been used for the construction and restoration of the Batalha Monastery in Portugal surface by PECVD from tetraethoxysilane (TEOS) as the reaction precursor, in capacitively coupled parallel-plate reactor. The thickness, morphologies and chemical properties of the deposited film were characterized by attenuated total reflectance -Fourier transform infrared (ATR-FTIR) spectroscopy and scanning electron microscopy (SEM+EDS). Laboratory simulated decay and natural aging tests were implemented to evaluate the protective effect of the deposited micron-size SiO_x thin films. Results suggested that, due to the good barrier effect, SiO_x films were able to isolate the stones from aggressive acidic solution, thus reducing possible dissolution-related damage. Natural aging tests proved that SiO_x thin films were also able to inhibit to a high extent bio-colonization while, at the same time reducing soiling of the stone appearance. Durability and wetting property of this SiO_x thin film were preliminarily assessed. This research tested, for the first time, the feasibility of applying micron-size SiO_x film quickly and directly via cold plasma deposition and its versatile protection performance on carbonate stone.

1. Introduction

Ornamental Stones in buildings and monuments in urban environments are exposed to the risk of significant decay as a consequence of anthropically and naturally produced agents [1–6]. The Batalha Monastery (also officially known as the "Mosteiro de Santa Maria da Vitoria") located in central Portugal near the city of Leira, has been included in the list of UNESCO World Heritage sites since 1983. Several local quarries provided the oolitic limestones for the construction of the monastery in 1386 and as well for the restoration programme in 1834 [7,8]. Over a century after the last large-scale restoration intervention, the Batalha Monastery is today showing a high degree of stone decay (Fig. 1), due not only to atmospheric pollutants from vehicular traffic sources (the Portuguese national highway IC2 - N1 runs around 50 m west to the building [9]) but also to bio-deterioration processes, which are known to play an ever-increasing role in stone decay in both urban and rural environments [3–6,10,11]. The intrinsic characteristics of these oolitic limestones under investigation, in particular porosity distribution, presence of cracks along the oolites and chemical behaviour of this sedimentary carbonate rock simultaneously facilitate the fast decay of the stone [10].

As widely studied, acid rain and biodeterioration processes can result in severe decay to building stone in urban environments, due to the burning of sulphur-containing fossil fuels for domestic and industrial purposes [12,13], the emissions of organic pollutants from vehicular traffic [5], the use of phosphate fertilizers [14], dry/wet cycles [15] and dry-wet deposition of windborne microorganisms [16], particulate matter and gaseous aerosols [17]. In order to enhance the resistance against environmental attack, restore the stone mechanical integrity and avoid the onset of decay processes such as surface decohesion and flaking, a number of treatment products have been suggested for stone conservation applications with a view to increase the water repellence, consolidate and/or anti-microbial properties of the building stone [18,19].

* Corresponding author.
E-mail address: schiavon@uevora.pt (N. Schiavon).

https://doi.org/10.1016/j.culher.2024.10.001

Fig. 1. Batalha Monastery, Portugal. Limestone heavily affected by microbial deterioration and lichenous patinas.

The most commonly used treatment products are:

- Synthetic organic polymer systems as acrylic polymers, vinyl polymers, epoxies [20]. These products have been extensively used since the middle of 20th century for their ease of application and immediate efficacy. However, through the action of sunlight radiation or environmental chemical attack, these organic consolidants can undergo photo-oxidation and molecular modifications. For instance, when the Bologna Cocktail (a mixture of synthetic resins used for stone consolidation) undergoes photo-oxidative degradation, the acrylic component can form intermolecular and terminal double bonds and oxidized species like γ-lactones as a result of chain cross-linking / scission processes [21]. These modifications cause the formation of strongly cross-linked structures associated with colour change and loss of protective properties. Another non negligible drawback effect could be their irreversibility [22]. The most dangerous consequence is that water and soluble salts in porous substrates could induce the onset of salt crystallization decay processes behind the hydrophobic coating layer, thus leading to even further material loss and decay [23,24]. Lately, multi layered method which introduces both hydrophobic and hydrophilic layers was proposed by some researchers, to disperse the expansion stress near the interface, in order to prevent the damage caused by wet-dry difference in polymer conservation and salt crystallization [25].
- Inorganic materials, as alkaline silicates, silicon fluorides, alkaline earth hydroxides (calcium, strontium and barium hydroxide). They have higher physical-chemical compatibility with stone substrates than polymers, and may act as consolidants or anti-fungal agents [26]. $Ba(OH)_2$ and $Ca(OH)_2$ based methods are specific for consolidating carbonate stones (i.e., limestone and marble) which do not harm the substrate, though, they do not have high penetration depth and take a long time to convert to $BaCO_3$ and $CaCO_3$ [27]. Lime water suspension is a traditional stone treatment, now nano-lime suspensions have been developed for better penetration and faster carbonation process [28,29]. AmO_x (ammonium oxalate) could passivate the calcite stone surface by converting $CaCO_3$ or $CaSO_4$ into CaC_2O_4, thus acting as a neutral de-sulphating agent [23]. $(NH_4)_2HPO_4$ is similar to AmO_x, with more uniform consolidating effect, low colour variation and non-toxicity [30]. Diammonium hydrogen phosphate (DAP) has also been proposed as consolidant which is able to penetrate into stone for >2 cm and to form hydroxyapatite by reacting with calcite in carbonate stones, thus increasing the stone dynamic elastic modulus and tensile strength with the calcium phosphate precipitates filling microcracks and pores. The reaction is written below and occurs in two days and can be realized in situ [31].

$$10CaCO_3 + 5(NH_4)2HPO_4 \rightarrow Ca_{10}(PO_4, CO_3)_6(OH, CO_3)_2 + 5(NH_4)2CO_3 + 3CO_2 + 2H_2O$$

The development of nano-technology as well contributed to stone heritage conservation. Nanoparticle-based consolidants are now commonly applied by restorers. For instance, nano $Ca(OH)_2$ dispersed in alcohol replaced the $Ca(OH)_2$ saturated solution that was once widely used to restore lithic cultural heritage overcoming the disadvantages such as low solubility andlow consolidation strength [32]. $Ca(OH)_2$/ZnO nanoparticles showed a good performance with regards to penetration depth while maintaining aesthetical and physical properties, while SiO2 achieved good results

in penetration test in their application on carbonate stones [33]. It was found that the contact strengthening is related to particle coordination (the number of adhesive bonds that each particle can form), thus explained the reason why small nanoparticles can increase cohesion in consolidation [34].

- Silane: tetraethoxysilane (TEOS) and methyltrimethoxysilane (MTMOS) have been both used to consolidate dense and compact carbonate stones by filling veins and small cracks, and as protective surface varnishes against environmental air pollution and acid rain [35]. TEOS could be applied for consolidating natural stone, including sandstone, granite and historical renders. The hydrolysis of alkoxy groups of TEOS splits off ethanol molecules, and the unstable intermediate silanol s –Si–OH are condensed to amorphous silica gel which functions as stone consolidant via hydrolysis reaction as follow [35,36]:

$$Si(OR)_3OH + OH^- \rightarrow Si(OR)_3O^- + H_2O$$

with the ethoxy groups (-OC_2H_5) progressively being replaced by hydroxyl groups (-OH). When hydroxyl groups of different molecules start to react:

$$Si(OR)_3O^- + Si(OH)_4 \rightarrow (OR)_3Si - O - Si(OH)_3 + OH^-$$

The cross-linking reactions are:

$$H - O - \left[Si(CH)_2\right] - OH + Si(OC_2H_5)_4 \rightarrow$$
$$= \left[2O = Si = 2\left[O - Si(CH_3)_2\right]_n\right] = 2(OH)$$

TEOS may be applied by sol-gel, however due to the capillary force, the gel always tends to develop cracks during drying [37]. To avoid such damages, several hybrid consolidants based on TEOS have been formulated such as TEOS-HDTMS xerogels, TEOS-colloidal-silica-PDMS-OH, TEOS/PDMS-OH/CTAB, GPTMS mixed with silica nanoparticles etc. [24,38,39,40]. Generally speaking, the modified gel / hybrid silane-inorganic particles are more stable and consequently the coating shows better protective performance, higher resistance to acid attack and salt weathering, even more, provides new protective features. For example, TEOS-FAS (1H,1H,2H,2H-perfluorooctyltriethoxysilane) sol solution deposited on marble achieved superhydrophobicity and water repellency, which is a durable and promising coating for stone protection [41]. The SiO_2 nanoparticles added in alkoxysilane-based consolidant improved its mechanical behaviour and drying time, forming a compact SiO_2 xerogel structure that filled the spaces between mineral grains, despite of the risk of over consolidation [42]. Nanolime modified by dimethyloctadecyl ammonium chloride showed durable antifungal effects without sacrificing the consolidation function [43]. Nanocomposites consisting of TEOS with nano-SiO2 and TiO2 particles significantly reduce the shrinkage and cracking comparing to pure TEOS stone consolidant [44].

The application methods of protective products on stones includes brushing, capillary absorption and immersion, spraying, nebulization, runoffs and drops. The choice of application methods depends on a complex combination of variables such as the size of treated areas, the expected penetration depth, evenly distribution, repeatability and accuracy [45]. During the 90′s, it was found that SiO_2-*like* film could be successfully deposited by plasma-enhanced / thermally-activated chemical vapor deposition (PECVD / TACVD), not on stone but on silicon wafer substrates, according to the following reaction [46]:

$$Si(OC_2H_5)_4 + 8O^{3+} \rightarrow SiO_2 + 10H_2O + 8CO_2$$

Substrate heating was required in film deposition to achieve acceptable electrical properties during the process [47,48]. In the last decade, advancement in organosilicon-based PECVD in oxygen and argon atmosphere, under capacitively coupled radio frequency plasma power source have been forthcoming: the deposition of SiO_x thin film could now be operated in low temperature plasma conditions, as opposed to high temperature plasma not suitable for Cultural Heritage assets nor for portable apparatus [49,50]. After the success in depositing SiO_x thin film on silver-based alloy and other metallic artefact as aesthetic coatings with corrosion protection properties [51,52], PECVD diamond-like carbon (DLC) coating was also applied on bronze as hydrophobic barrier [53]. Therefore, protective coating on cultural heritage works via PECVD methodology is worthy of in-depth exploration, especially its application on different materials.

2. Research aims

The application of PECVD coating had been restricted to using silicon wafers on metals in the past, but its use on stone heritage artefacts as protective coating has never been assessed, with the exception of one published article reporting hydrophobicity modification of quarry stone surface by plasma-polymerized hexamethyldisiloxane (PPHMDSO) [54]. The aim of the current study was fourfold:

1) to test the feasibility of a new technical route of applying TEOS on stone surface as protective coating film via PECVD in lab condition;
2) to evaluate various protective performance of the plasma deposited SiO_x thin films against several environmental decay factors, by means of laboratory simulation and field exposure, including acid attack, microbial-colonization and colour changing tests;
3) to discuss the advantages/feasibility of using PECVD as a technique to apply a protective thin SiO_x film on carbonate building stones;
4) to suggest an alternative methodology for the protection of the Batalha Monastery monument limestone and to identify the parameters that need to be taken into account in view of its future application in real contexts.

3. Materials and methods

3.1. Sample collection, pretreatment and SiO_x film deposition

Limestone samples used in this study came from three quarries (Valinho do Rei, Pidiogo, Cabeço do Roxo) located nearby the monument under investigation, which were reported as the sites of provenance of the material used for the construction and restoration of the Batalha Monastery [8]. They are oolitic limestones from late Jurassic age consisting of 97∼99 % calcite and 1 % of quartz minerals [8]. The porosity of Valinho do Rei limestone is 1.1 %, and that of Pidiogo limestone and Cabeço do Roxo limestone is 16.9 % and 14.9 % respectively [55]. These limestones blocks were cut into specimens of three different sizes: 2.5 × 2.5 × 1 cm; 2.5 × 2.5 × 0.3 cm; 5 × 5 × 1 cm. The surfaces to be subjected to PECVD were polished with 600# sand paper, washed by distilled water, dried in oven at 60 °C, and then cleaned with 97 % ethanol.

SiO_x thin films were deposited by PECVD in a capacitively-coupled parallel plate reactor. The reactor was used in a two-electrodes configuration; the upper electrode was connected to a radio frequency (13.56 MHz) power supply through an impedance matching unit, while the bottom electrode was connected to the ground. Gas and TEOS vapor flow rates were controlled by means of a mass-flowmeter and vapor system and inserted in the chamber through the upper electrode which acted as a shower electrode; a throttle valve allowed the working pressure regulation

Table 1
Sample information, deposition condition and experiments routines (*standard cubic cm per minute).

PECVD conditions				
Samples	Ar / O_2 gas flow (sccm*)	TEOS flow (sccm)	Input power (W)	Time (min)
Group A (A1, A2, A3)	Ar 80, O_2 20	1 sccm	100	20
Group B (B1, B2, B3)	Ar 80, O_2 20	2 sccm	100	40
Group C (C1, C2, C3)	Ar 80, O_2 20	2 sccm	200	40
Group D (D1, D2, D3)	Ar 80, O_2 20	2 sccm	200	20
Group E (E1, E2, E3)	Ar 50, O_2 50	2 sccm	200	40
Group F (F1, F2, F3)	Ar 50, O_2 50	2 sccm	200	20
Experimental protocol				
Samples	A1, B1, C1, D1, E1	A2, B2, C2, D2, E2		A3, B3, C3, D3, E3
Sample size	2.5 × 2.5 × 1 cm	2.5 × 2.5 × 0.3 cm		5 × 5 × 1 cm
Experiment methods	FTIR → Microbial incubation → SEM → Wipe clean → SEM	(i) Resin embedded → Cut → SEM+EDS (cross-section) (ii) SEM+EDS (surface) → Weighted → Acid rain simulation → Weighted → SEM+EDS		Colorimetry → Outdoer field exposure → Colorimetry → OM
Quarry source	Valinho do Rei	Pidiogo		Cabeço do Roxo

measured by a baratron capacitance manometer. SiO_x depositions tests were performed in plasma fed with TEOS/O_2/Ar mixture at different ratios, by varying the input power and the deposition time, at the floating plasma temperature (T < 60 °C) and 100 mTorr of pressure. The experimental parameters were optimized from deposition test on silicon wafers, guaranteed to form thin film of 0.3–1.0 um thickness, then selected as operating parameters for the deposition on limestone samples, as reported in Table 1. To ensure comparability, each experimenting protocol was performed on samples from identical quarry: the corresponding experimental design after PECVD is as well listed in Table 1.

3.2. Characterization of SiO_x thin films

The SiO_x coated samples were characterized by ATR-FTIR in order to define the chemical composition of the coating deposited on the limestone surface. The FTIR spectra were recorded by Perkin Elmer Spectrum 2000 FTIR spectrometer (Perkin Elmer, Norwalk, CT, USA) equipped with a single reflection attenuated total reflectance (ATR) accessory. For each sample, 16 scans were recorded with resolution of 4 cm^{-1}.

The coated specimens of size of 2.5 × 2.5 × 0.3 cm were impregnated with resin and cut for cross-section observation. Scanning electron microscopy coupled with energy dispersive X-ray spectrometry (SEM+EDS) was carried out using a Hitachi S3700N (Tokyo, Japan) SEM coupled to a Bruker (Karlsruhe, Germany) XFlash 5010 SSD Detector system. The samples were characterized at a chamber pressure of 40 Pa, without any sample preparation, under an accelerating voltage of 20 kV, with a working distance 10–20 mm and using the BSEM mode.

3.3. Acid rain weathering, microbial colonization and field exposure tests

3.3.1. Acid rain weathering test

Samples were set in a funnel at tilt angle of 45°, while a H_2SO_4 solution at pH=3.5 was allowed to drip on the specimen surface with a flow rate of 5 mL/min. After every 50 mL of acid solution, the samples were dried in a laboratory oven at T = 60 °C for 1 h, the acid dripping was repeated for 5 cycles. A total volume of 200 mL of the sulfuric acid solution was dripped on each sample, then the specimens were washed in ultrasonic bath in distilled water, dried and weighted in order to evaluate the weight loss due to the acid rain attack and finally observed under the SEM-EDS before and after ultrasonic washing (same settings as in Section 3.3) [24].

3.3.2. Lab-simulated microbial contamination tests

For bacterial and fungal growth, a malt extract (ME) medium was prepared with 20 g/L malt extract, 20 g/L glucose and 1 g/L peptone, then sterilized in autoclave for 20 min at 120 °C and 1.5 bars. 1 mL of saline medium which contains the collected microorganism from the Batalha Monastery site was added into 500 mL ME medium, this culture was then kept in an incubator for 72 h with controlled temperature of 28 °C and orbital agitation at 150 rpm. 1 mL of mixed culture was used to inoculate each limestone tablet, microorganisms in their culture media were spread on the specimen surface. Then all limestone tablets were incubated in the ARALAB Plant Growth Chamber for 15 days, with controlled temperature at 28 °C, humidity at 81.0 % RH, and 10 % illumination of 4 × 18 W fluorescent. [56].

3.3.3. Outdoor field exposure tests

Stone tablets, 5 × 5 × 1 cm in size, uncoated and coated with SiO_x thin film were exposed on the roof of the Batalha Monastery facing south from 9th June to 10th October 2021 (Fig. 2). The tablets were collected after three months' exposure and observed under optical microscope. By means of the Datacolour CHECK II PLUS Spectrophotometer, the colour change of sample surfaces before and after outdoor exposure was evaluated. The result was illustrated using the CIELab Colour Space system.

3.4. Alteration in vapor permeability and wetting property

3.4.1. Water vapor permeability test

To assess vapor permeability, limestone samples, uncoated and coated with SiO_x thin film, were fixed and sealed with Parafilm on the top of identical glass containers partially filled with water, never in contact with the samples bottom. The containers with the samples were then placed in an oven at T = 60 °C for 7 days, and weighted every 24 h. Linear regression between weight change and time was made by Excel, the water permeability of each sample was extrapolated by the slope of the accordingly linear function [41] and [57].

3.4.2. Water contact angle measurements

Water contact angle measurements were performed using the sessile drop method at room temperature, with double distilled water (γ = 72.8 mN/m) [58]. The measurement was carried out by a Kruss DSA10 instrument (Hamburg, Germany) equipped with a video camera.

Fig. 2. Uncoated and SiO_x deposited stone samples placed on the roof of Batalha Monastery (from left to right, 1st and 3rd covered with SiO_x thin film, 2nd and 4th uncoated).

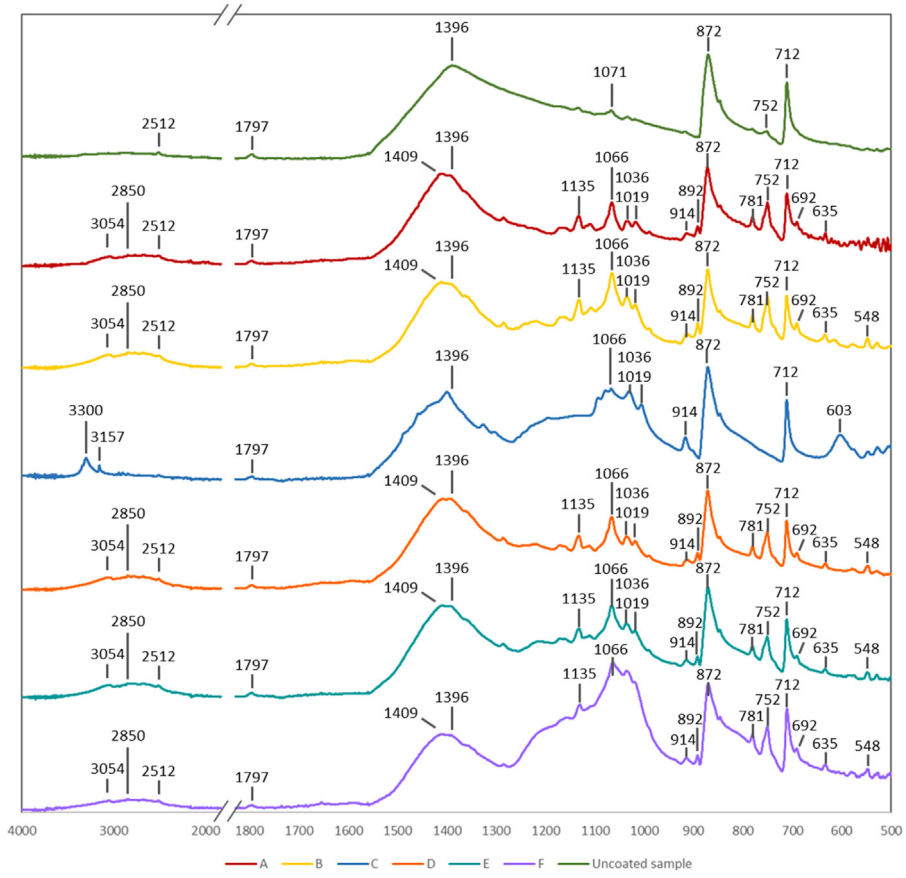

Fig. 3. ATR-FTIR spectra recorded on an uncoated sample and on SiO_x thin film coated samples (A1, B1, C1, D1, E1, F1) in the conditions listed in Table 1.

4. Results and discussion

4.1. SiO_x thin film characterization

FTIR analysis were performed in order to study the effect of input power and the composition of gas mixture on the chemical structure of the deposited layer. Fig. 3 shows the ATR-FTIR spectra recorded on the SiO_x film coated limestone samples (A1, B1, C,1 D1, E1, F1) under the experimental conditions shown in Table 1, compared with the spectrum of the uncoated sample surface. Limestone without film deposition was characterized by absorption bands at wavenumbers 2514 cm^{-1}, 1795 cm^{-1}, 1396 cm^{-1}, 872

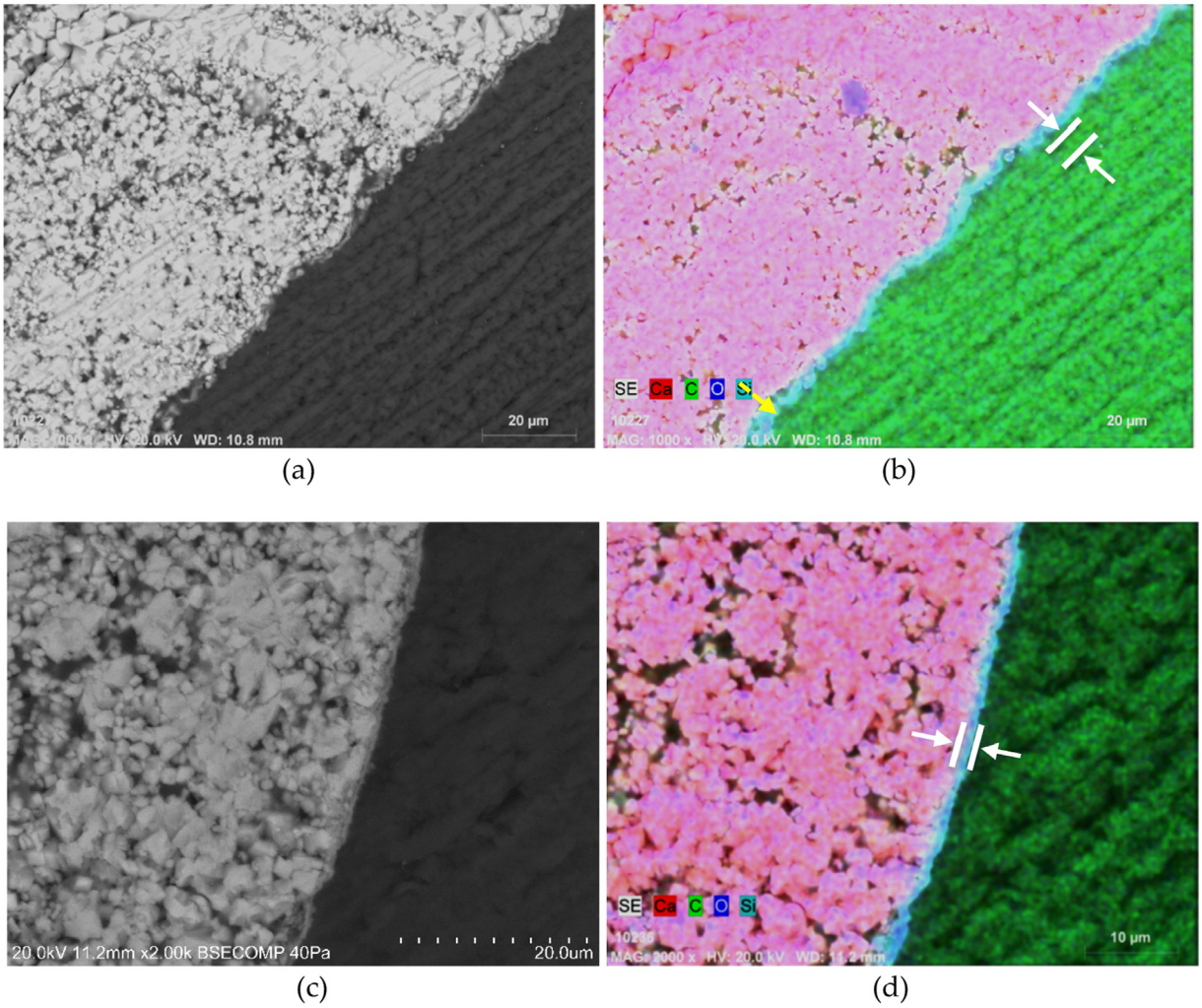

Fig. 4. SEM image and EDS map of the cross-section of a SiO_x thin film deposited on oolitic limestone specimens, B2 (a and c) and E2 (c and d).

cm^{-1}, 712 cm^{-1}, which are typical bands of low-magnesium calcite, while the small peak at 1072 cm^{-1} can be attributed to the presence of minor quartz [RRUFF ID: R040070.1] [59,60,61]. FTIR bands at 1070 cm^{-1} and 782 cm^{-1} can be attributed to quartz [RRUFF ID: R040031.1]. On the SiO_x deposited samples, a broad Si-O symmetric stretching peak at 1066 cm-1 was detected [62]. The broad curve between 3300 and 2200 cm^{-1} relates to O–H stretching [63]. The peak at 1132 cm^{-1} is associated with the C–O stretching bond [64], and the peak at 781 cm^{-1} is attributed to the stretching mode of the transversal optic phonons (SiC(TO)) and the deformation of Si-CH_3 and a simple stretching of Si-C bond [65,66]. The experimental findings confirm the presence of SiO_x film on the limestone surface, with some of the $-OCH_3$ groups unreacted from the TEOS precursor. In particular, by increasing the input power and the oxygen content in the plasma, an increase in the features of Si-O-Si is observed, while the presence of Si-C bonds in the film structure decreases, as the increase of power favours the removal of both associated and isolated hydroxyl groups during the deposition process [67].

Fig. 4 shows the SEM images of the cross-section of the SiO_x film deposited limestone surface, as two examples B2 and E2 (Table 1). The SiO_x films are continuous with a high adaptability to the substrate morphology. Unlike that on silicon wafers where the film thickness changes according to the time of deposition, input power and TEOS flow, here on the limestone tablets the film thickness is constantly around 2 μm (white marks in Fig. 4b and d) in all deposition conditions. Despite being deposited under higher input power, higher TEOS flow speed and longer time (condition E towards B in Table 1), the thin film seems to have smoother and denser shape.

Since the Si element is represented as light blue and limestone is of pink red in the EDS mapping, a rather thin layer of purple colour beneath the SiO_x film (pointed by yellow arrow in Fig. 4b) thus could be recognized as the overlapping of Ca and Si elements, which means that the penetration depth of the SiO_x film on the limestone substrate is no >1 μm.

4.2. Wetting property and vapor permeability

The deposited SiO_x film does not seem to provide the substrate with water repellent properties. As a matter of fact, the water contact angle measurement test could not be carried out normally on the limestone samples because for both uncoated and coated tablets, the water droplet was not able to maintain a spherical shape and was absorbed by the substrate within few seconds. In fact, the Si-OH bonds in the deposited SiO_x film with hydroxyl (-OH) groups are recognized as hydrophilic [68], thus it is reasonable this SiO_x film didn't show hydrophobic character.

The weight loss with time due to water vapor permeability is shown in Fig. 5 for uncoated and PECVD samples. Linear regression

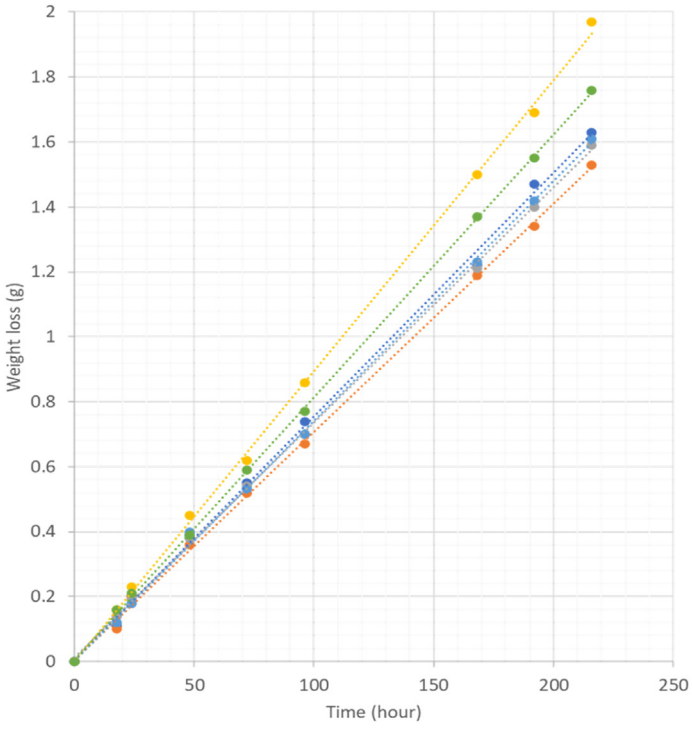

Sample	Vapour permeability (g/hour)
B	0.0075
C	0.0070
D	0.0072
E	0.0089
F	0.0074
Uncoated sample	0.0081

Fig. 5. Weight loss related to time by water vapor permeability.

was made to fit the rate of weight change of each sample, and the corresponding slope represents the vapor permeability rate (g/h). In order to obtain the relative ratio of permeability, the value of each sample was divided by one. All the coated samples had a permeability rate change <14 %, in particular samples deposited under condition B and F of had only 7 % and 9 % difference with respect to the uncoated specimens. Sample coated under condition E showed, unexpectedly, higher permeability than uncoated samples: this might be attributed to the presence of cracks on the stone surface.

A strong decrease in water permeability could remarkably increase the risk of water accumulation underneath the stone surface, leading to decay caused by dry–wet and freeze–thaw cycles [25]. Temperatures in Batalha can go below 0 °C during winter, hence, to limit such risk is advisable, especially in the case of monuments and artefacts located outdoor in non-tropical regions. By SiO_x thin film coating, with a water vapor permeability reduced to <15 % or even to <10 %, such changes are acceptable [70], this would avoid potential damage caused by internal moisture condensation [71].

4.3. Acid rain weathering effect test

In Fig. 6, the SEM-EDS images of the surfaces of uncoated limestones after acid rain test are shown. It can be seen that in the area of micrite and sparite crystalline cement, several voids appeared, and small crystal grains with diameter < 10 μm size were precipitated (Fig. 6a and c, circled by blue dash lines). The outline of oolites also became discontinuous (Fig. 6b), some of the oolites even losing their outline (circled by red dash lines). Small grains in Fig. 6c are proved to be sulphur-rich (d) in the EDS mapping, confirming the precipitation of gypsum crystals ($CaSO_4 \cdot 2H_2O$).

In the case of SiO_x coated specimens, the acid rain test led to different results. The SEM images in Fig. 6e and f showed that the SiO_x thin film is essentially unaffected by the acid rain test. Fig. 6f showing a homogenous distribution of Si in the EDS maps. In areas where precipitation of S-rich acicular crystals is visible, there is the loss of Si-signal in the EDS mapping (yellow circles in Fig. 6g and h). This is evidence of the protective effectiveness of the SiO_x thin film, because where the coating was cracked and lost, which could also be seen in the BSE photo (white dash frame in Fig. 6g, the stone substrate reacted with the sulfuric acid and produced acicular calcium sulphate crystals [69], whereas in areas covered by the coating no sulphation occurs.

After ultrasonic cleaning and drying, the specimens were weighted in order to obtain the mass loss due to acid rain dissolution reactions. The uncoated samples recorded a weight loss of 0.04 g under the effects of 200 mL H_2SO_4, while in the case of all the SiO_x deposited samples, only a weight loss of 0.01–0.02 g was observed. This demonstrates that the SiO_x film was able to hinder the contact between the limestone and the acid to a certain extent, thus reducing the dissolution and mass loss of $CaCO_3$.

4.4. Resistance to microbial colonization

For uncoated limestones, after a 14-days incubation, the microorganisms have already aggregated into colonies with size up to 0.8 mm (circled by dash frame in Fig. 7a). In some areas, the bio-colonization has occupied the whole oolitic framework (circled by dash frame in Fig. 7b). By wiping the surface with air-laid paper and distilled water, large areas of bio-colonization were removed but a number of microbial colonies around 100–200 μm in diameter still persisted (blue frames in Fig. 7c), as well as some bar-shaped fungal spores (frames in Fig. 7d). While for the SiO_x thin film coated limestones, in most areas the microorganisms grouped into agglomeration spots of around 50∼100 μm in size (Fig. 7e and f), with larger microbial communities also present in specific areas but less abundant than those found on the uncoated limestone samples (Fig. 7e). After wiping the surface with distilled water and air-laid paper, most of the colonies were removed with only a few colonies of <50 μm in size left at the boundary or within oolites (dark spots framed by dash lines in Fig. 7g and h. This may be

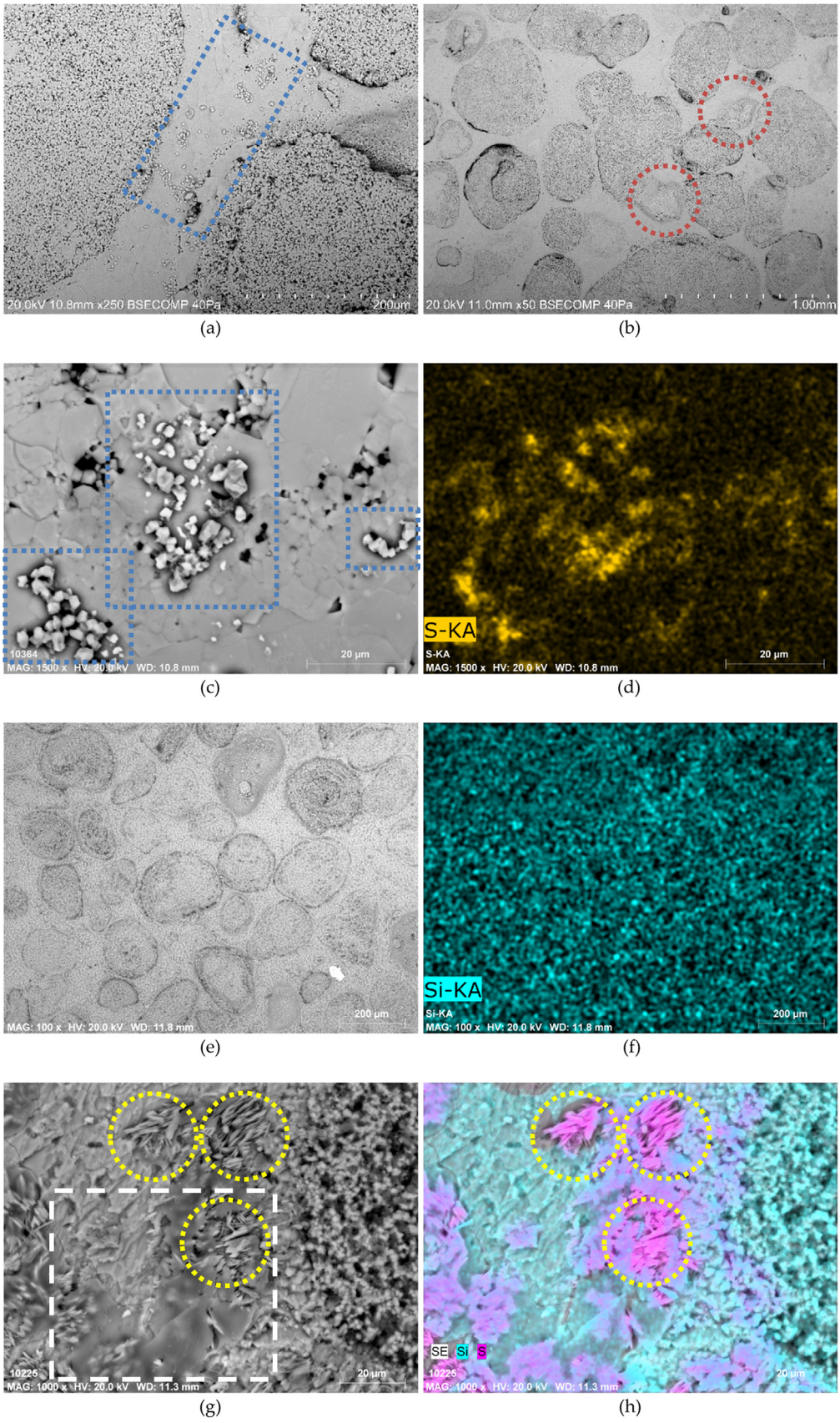

Fig. 6. SEM-EDS images of uncoated sample and the SiO_x deposited sample F2 after the acid rain test. (a, b, c). BSEM-EDS images of uncoated limestone samples after acid rain test; (d): Sulphur elemental map of image (c). See text for further details; (e) general view of the surface which appears unaffected by the acid test; (f) Si elemental map referring to image (a) showing homogeneous distribution of SiO_x film; (g). Area with visible cracks in the coating (yellow circles) and corresponding Si and S elemental map (h).

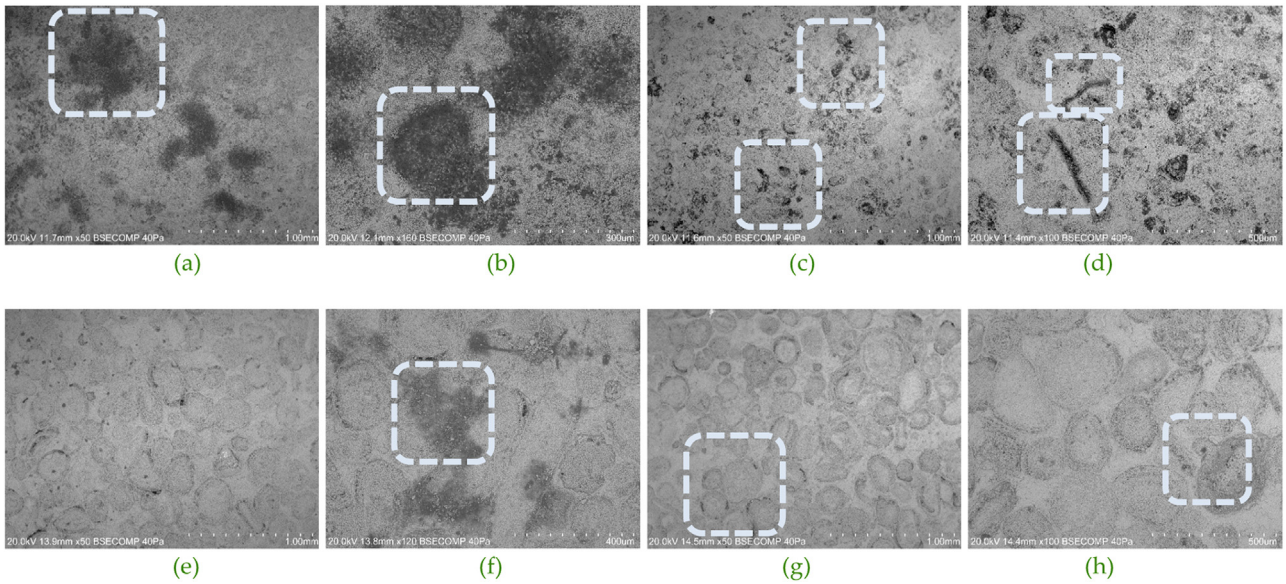

Fig. 7. SEM of the uncoated stone sample and SiO_x deposited stone sample after microbial-incubation. (a and b). uncoated stone after incubation and (c and d). then wiped by airlaid paper with distilled water; (e and f). SiO_x deposited stone after incubation and (g and h). Wiped by airlaid paper with distilled water.

Table 2
L*a*b* coordinates of the samples before and after exposure on the roof of Batalha Monastery.

	Samples	Coordinates	L	a	b
Before exposure	Uncoated sample	value	89.64	1.95	8.29
	Sample deposit with SiOx	value	89.36	2.09	8.95
	thin film (D3)	Δ	−0.28	0.14	0.66
After exposure	Uncoated sample	value	80.96	1.79	7.75
		Δ	−8.68	−0.16	−0.54
	Sample deposit with SiOx	value	88.70	1.46	6.72
	thin film (D3)	Δ (comparing to original stone before exposure)	−0.94	−0.49	−1.57
		Δ (comparing to SiOx deposited stone before exposure)	−0.66	−0.63	−2.23

due to the higher microporosity associated with oolitic structure. SiO_x coating might be absent in some areas where the substrate showed missing oolite grains, thus giving opportunity for microorganism colonization. As a general observation, the SiO_x thin film reduced the risk of microbial colonization and moreover, bacterial and fungal colonies eventually developed on the surface could be easily wiped away using just distilled water.

4.5. Outdoor field exposure tests

Limestone tablets exposed on the roof of the Batalha Monastery were observed under stereo microscope (Fig. 8). On uncoated specimens, black spots probably of biological origin grew extensively on the surface, their density higher than 600 spots/ mm^2 (Fig. 8a and b); meanwhile on the SiO_x coated samples, the black spots density is definitely lower than 80 spots/mm^2 (Fig. 8c and d).

Such different behaviour is also reflected on the colour of the limestones, as shown in Table 2. In the case of the uncoated specimens, after outdoor exposure the change in lightness ΔL reached −8.68, this means that the sample became darker. In the case of SiO_x coated samples, ΔL was −0.94, thus confirming that the SiO_x thin film was able to significantly preserve the bright appearance of the stone. According to the red/green and yellow/blue index, the uncoated specimens showed $a = 1.79$ and $b = 7.75$, meanwhile the SiO_x coated specimens showed $a = 1.46$ and $b = 6.72$, comparing with the original stone before exposure ($a = 1.95$ $b = 8.29$), it can be indicated that the uncoated sample turned more red and yellow component. The red-yellow colour combining with darkening will end up in the orange – brownish look, that might be a reason the deteriorated monastery facades has an orange-brownish appearance.

It is also noteworthy that, before field exposure, the uncoated and SiO_x deposited samples showed a slight difference in colour index (ΔL = −0.28, Δa – 0.14, Δb = 0.66), which means the deposited film did not significantly change the appearance of the stone surface, but it helped the stone to maintain brightness after exposure.

In summary, the interaction with solar irradiation, the contamination from urban gaseous and particulate air pollutants and microbial colonization, changed the aesthetic appearance of uncoated limestones, meanwhile the deposition of SiO_x thin films is able to preserve the limestone surface unaltered.

4.6. SiO_x thin film durability

The durability of the SiO_x films was evaluated by SEM-EDS (Fig. 9). On the samples submitted to the acid rain test, most part of the SiO_x film remained flawless, except in some area holes of 10–20 μm in size were lost within the film that is evident in the Si EDS maps (Fig. 9b), which was caused by the detachment of oolites. In the case of the outdoor filed exposed limestone tablets, the SiO_x coating remained almost intact.

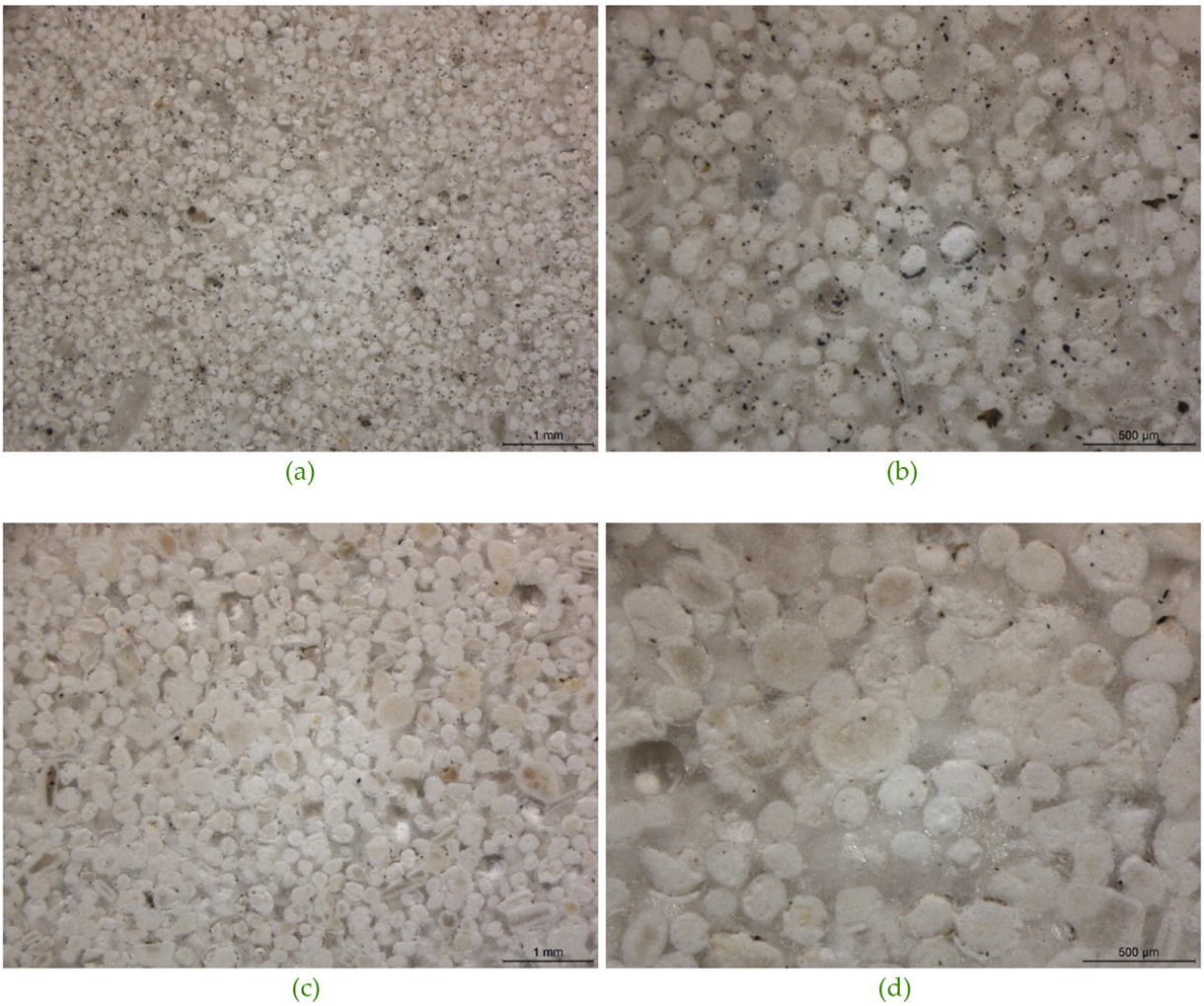

Fig. 8. Sample tablets after three months of field exposure. (a and b). Sample without SiO_x coating; (c and d). Sample D3 with SiO_x thin film deposited.

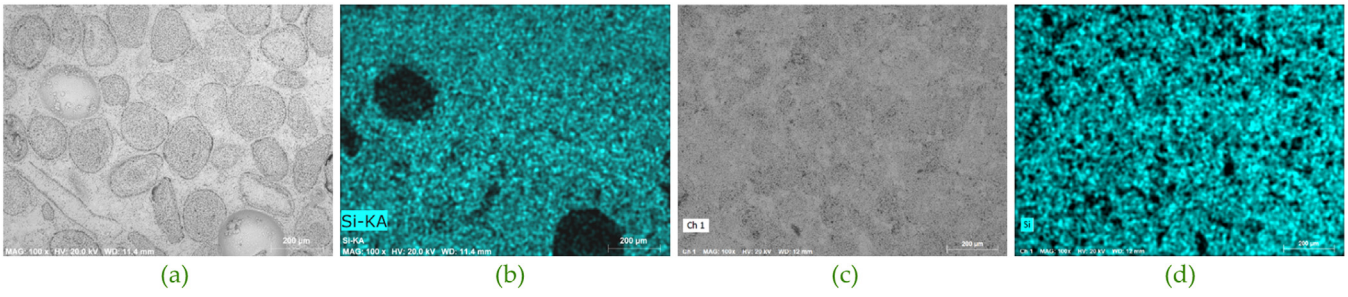

Fig. 9. SEM-EDS of the acid attacked and field exposed samples. (a) BSE of the surface attacked by acid; (b) Si-element mapping of (a); (c) BSE of the exposed stone surface; (d) Si-element mapping of (c).

5. Conclusions

In this study the protective effectiveness of PECVD SiO_x thin film on limestones used in construction and restoration of the Batalha Monastery Portuguese UNESCO WH-listed monument was assessed by means of acid rain weathering test, outdoor exposure tests and microorganism colonization activity measurements. Water vapor permeability changes induced by the surface coating were also investigated. The PECVD deposited SiO_x thin films were able to prevent the contact between acid solutions and the stone surface, as well as in slowing down microbial colonization and growth. The SiO_x thin film did not seem to increase, though, the hydrophobicity of the stone, while achieving good results in maintaining its vapor permeability. On a compact and low porosity substrate, PECVD SiO_x thin film achieves a good performance in terms of resistance against environmental weathering. This technique may be suitable, in particular, for applications to artefacts outdoor made in stone, or even ceramic and other inorganic materials.

The overall protective effectiveness of this coating is significant and its application is of noteworthy interest as confirmed in a recent study that shows the feasibility of using atmospheric pressure plasma to deposit SiO_x thin film from different monomers (TEOS, HMDSO) [74]. According to the experimental results, it can

be demonstrated that PECVD SiO_x thin films may be successfully used in stone protection as they contribute to: a) prevent the microbial contamination and colonization on the stone surface; b) protect the stone substrate from aggressive environmental agents such as acid solution; c) maintain the aesthetic appearance/colour of the stone and limit darkening of the stone façade (soiling).

PECVD SiO_x thin films do not behave as other commonly used consolidants and/or protective varnishing, as they do not fill up the already existing holes or cracks, nor they consolidate the flaking and detached stone fragments. However, SiO_x films do not impact significantly on the permeability of original limestones, whereas polymeric material usually reduce of 30 %–50 % the stone permeability [72,73], and consequently SiO_x films are able to prevent water condensation-related decay [70,71]. The advantages of SiO_x coatings deposited by PECVD are related to the short operation time: as a matter of fact, a crack-free film could be obtained in only 20–40 min of deposition. On the other hand, the formation of SiO_x coating produced by sol-gel or chemical solution reaction may require months during which cracks in the layer could be induced [36]. Although there is still a dimensional limitation of the objects/artefacts that can be treated in relation to the chamber size, PECVD is still a viable alternative for protecting small stone artefacts. The results of this research can also provide the basis also applicable for other work, for instance, protective coatings can be deposited on stone façade when proper atmospheric plasma devices will be designed.

In fact, further research is currently being proposed for funding on the development of low-cost, portable and easy-to-use plasma instruments that could be used by conservators/restorers for the deposition of thin SiO_x films on outdoor stone facades, buildings, statues, monuments and Cultural Heritage multi-matric assets. A recent study showing the feasibility of depositing SiO_x thin film on different metals from different monomers (TEOS, HMDSO) in outdoor conditions [74], giving value and probability to the large scaled application of this conservation methodology.

Funding

This research has received funding from the European Union's Horizon 2020 research and innovation programme under the Marie Skłodowska-Curie grant agreement No 766311.

Acknowledgments

The research presented in this paper was carried out mainly using data collected at Universidade de Évora, Politecnico di Torino and Direção-Geral do Patrimonio Cultural, as part of H2020-MSCA-ITN-2017, ED-ARCHMAT Project (ESR1).

References

[1] V. Fassina, Environmental pollution in relation to stone decay, Durab Build Mat 5 (1988) 317–358.
[2] B. Graue, S. Siegesmund, P. Oyhantcabal, et al., The effect of air pollution on stone decay: the decay of the Drachenfels trachyte in industrial, urban, and rural environments—a case study of the Cologne, Altenberg and Xanten cathedrals, Environ Earth Sci 69 (2013) 1095–1124, doi:10.1007/s12665-012-2161-6.
[3] N. Schiavon, T. De Caro, A. Kiros, I.E. Parisi, C. Riccucci, G.E. Gigante, A multi-analytical approach to investigate stone biodeterioration at a UNESCO world heritage site: the volcanic rock-hewn churches of Lalibela, Northern Ethiopia, Applied Physics Part A 113 (4) (2013) 843–854, doi:10.1007/s00339-013-7757-5.
[4] N. Schiavon, Kaolinisation of granite in an urban environment, Environm Geol 52 (2007) 399–407, doi:10.1007/s00254-006-0473-0.
[5] N. Schiavon, G. Chiavari, D. Fabbri, Soiling of limestone in an urban environment characterized by heavy vehicular exhaust emissions, Environm Geol 46 (2004) 448–456, doi:10.1007/s00254-004-1046-8.
[6] N. Schiavon, Biodeterioration of calcareous and granitic building stones in urban environments, in: S. Siegesmund, T. Weiss, V.A. Vollbrecht (Eds.), Natural stone, weathering phenomena, conservation strategies and case studies, Geological Society of London Special Publication, London, United Kingdom, 2002, pp. 195–206. https://doi.org/10.1144/GSL.SP.2002.205.01.15.
[7] JC. Vieira da Silva, The monastery of Batalha, Scala Books, London, 2007 ISBN 978–1857593822.
[8] Y. Ding, J. Mirao, P. Redol, L. Dias, P. Moita, E. Angelini, S. Grassini, N. Schiavon, Provenance study of the limestone used in the construction and restoration of the Batalha Monastery (Portugal), Acta IMEKO 10 (1) (2021) 122–128, doi:10.21014/acta_imeko.v10i1.857.
[9] M. Marques, Desvio do trânsito é a melhor solução para o Mosteiro da Batalha, Diário de Notícias (2018) https://www.dn.pt/portugal/populacao-esta-contra-barreiras-junto-ao-mosteiro-da-batalha-e-pede-isencao-de-portagens-9028235.html.
[10] Y. Ding, C.S.C. Salvador, A.T. Caldeira, E. Angelini, N. Schiavon, Biodegradation and microbial contamination of limestone surfaces: an experimental study from Batalha Monastery, Portugal, Corros Mat Degradat 2 (1) (2021) 31–45, doi:10.3390/cmd2010002.
[11] L. Aires-Barros, M.J. Basto, A. Dionísio, A.E. Charola, Orange coloured surface deposits on stones from the Monastery of Batalha (Portugal) and from nearby historic quarries: characteristics and origins, Int J Restorat Build Monum 7 (5) (2001) 491–506, doi:10.1515/rbm-2001-5594.
[12] D. Camuffo, Acid rain and deterioration of monuments: how old is the phenomenon? Atmospher Environm Part B. Urban Atmosphere 26 (2) (1992) 241–247, doi:10.1016/0957-1272(92)90027-P.
[13] A.E. Charola, R. Ware, in: Acid deposition and the deterioration of stone: a brief review of a broad topic, 205, Geological society, London, special publications, London, 2002, pp. 393–406, doi:10.1144/GSL.SP.2002.205.01.28.
[14] V. Matović, S. Erić, A. Kremenović, P. Colomban, D. Srećković-Batoćanin, N. Matović, The origin of syngenite in black crusts on the limestone monument King's Gate (Belgrade Fortress, Serbia)–the role of agriculture fertiliser, J Cult Herit 13 (2) (2012) 175–186, doi:10.1016/j.culher.2011.09.003.
[15] G. Khanlari, Y. Abdilor, Influence of wet–dry, freeze–thaw, and heat–cool cycles on the physical and mechanical properties of Upper Red sandstones in central Iran, Bull Eng Geol Environ 74 (2015) 1287–1300, doi:10.1007/s10064-014-0691-8.
[16] R.D. Wakefield, M.S. Jones, An introduction to stone colonizing microorganisms and biodeterioration of building stone, Quart J Engineer Geol Hydrogeol 31 (4) (1998) 301–313, doi:10.1144/GSL.QJEG.1998.031.P4.03.
[17] K. Torfs, R. Van Grieken, Chemical relations between atmospheric aerosols, deposition and stone decay layers on historic buildings at the Mediterranean coast, Atmos Environ 31 (15) (1997) 2179–2192, doi:10.1016/S1352-2310(97)00038-1.
[18] C.A. Price, E. Doehne, Stone conservation: an overview of current research, Getty Publications, Los Angeles, USA, 2011.
[19] M. Favaro, P. Tomasin, F. Ossola, P.A. Vigato, A novel approach to consolidation of historical limestone: the calcium alkoxides, Appl Organomet Chem 22 (12) (2008) 698–704, doi:10.1002/aoc.1462.
[20] A. Ershad-Langroudi, H. Fadaei, K. Ahmadi, Application of polymer coatings and nanoparticles in consolidation and hydrophobic treatment of stone monuments, Iran Polym J 28 (1) (2019) 1–19.
[21] M. Favaro, R. Mendichi, F. Ossola, S. Simon, P. Tomasin, P.A. Vigato, Evaluation of polymers for conservation treatments of outdoor exposed stone monuments. Part II: photo-oxidative and salt-induced weathering of acrylic–silicone mixtures, Polym Degrad Stab 92 (3) (2007) 335–351, doi:10.1016/j.polymdegradstab.2006.12.008.
[22] M. Favaro, R. Mendichi, F. Ossola, U. Russo, S. Simon, P. Tomasin, P.A. Vigato, Evaluation of polymers for conservation treatments of outdoor exposed stone monuments. Part I: photo-oxidative weathering, Polym Degrad Stab 91 (12) (2006) 3083–3096, doi:10.1016/j.polymdegradstab.2006.08.012.
[23] M. Matteini, Inorganic treatments for the consolidation and protection of stone artefacts, Conserv Sci Cult Herit 8 (2008) 13–27, doi:10.6092/issn.1973-9494/1393.
[24] F. Xu, D. Li, H. Zhang, W. Peng, TEOS/HDTMS inorganic–organic hybrid compound used for stone protection, J Solgel Sci Technol 61 (2) (2012) 429–435, doi:10.1007/s10971-011-2643-0.
[25] H. Zhang, Q. Liu, T. Liu, B. Zhang, The preservation damage of hydrophobic polymer coating materials in conservation of stone relics, Progr Organ Coat 76 (7–8) (2013) 1127–1134, doi:10.1016/j.porgcoat.2013.03.018.
[26] A. Sierra-Fernandez, L.S. Gomez-Villalba, S.C. De la Rosa-García, S. Gomez-Cornelio, P. Quintana, M.E. Rabanal, R. Fort, Inorganic nanomaterials for the consolidation and antifungal protection of stone heritage, in: Advanced materials for the conservation of stone, Springer, Cham, 2018, pp. 125–149, doi:10.1007/978-3-319-72260-3_6.
[27] Croveri, P., Dei, L., Giorgi, R., & Salvadori, B. (2004). Consolidation of Globigerina limestone (Malta) by means of inorganic treatments: preliminary results. In *Proc. 10th Int. Congress on Deterioration and Conservation of Stone,* D. Kwiatowski & R. Lofvendahl, Stockholm (eds.) (pp. 463–470).
[28] P. D'Armada, E. Hirst, Nano-lime for consolidation of plaster and stone, J Architec Conserv 18 (1) (2012) 63–80, doi:10.1080/13556207.2012.10785104.
[29] C. Rodriguez-Navarro, A. Suzuki, E. Ruiz-Agudo, Alcohol dispersions of calcium hydroxide nanoparticles for stone conservation, Langmuir 29 (36) (2013) 11457–11470, doi:10.1021/la4017728.
[30] M. Matteini, S. Rescic, F. Fratini, G. Botticelli, Ammonium phosphates as consolidating agents for carbonatic stone materials used in architecture and cultural heritage: preliminary research, Int J Architec Herit 5 (6) (2011) 717–736, doi:10.1080/15583058.2010.495445.
[31] E. Sassoni, S. Naidu, G.W. Scherer, The use of hydroxyapatite as a new inorganic consolidant for damaged carbonate stones, J Cult Herit 12 (4) (2011) 346–355, doi:10.1016/j.culher.2011.02.005.

[32] Jinmeng Zhu, et al., Nano Ca $(OH)_2$: a review on synthesis, properties and applications, J Cult Herit 50 (2021) 25–42, doi:10.1016/j.culher.2021.06.002.
[33] Javier Becerra, Ana Paula Zaderenko, Pilar Ortiz, Basic protocol for on-site testing consolidant nanoparticles on stone cultural heritage, Heritage 2 (4) (2019) 2712–2724, doi:10.3390/heritage2040168.
[34] Joanna Dziadkowiec, et al., Cohesion gain induced by nanosilica consolidants for monumental stone restoration, Langmuir 38 (22) (2022) 6949–6958, doi:10.1021/acs.langmuir.2c00486.
[35] Rolf Snethlage, Katja Sterflinger, Stone conservation, in: Stone in architecture: properties, Durability, Springer Berlin Heidelberg, Berlin, Heidelberg, 2010, pp. 411–544, doi:10.1007/978-3-642-14475-2_7.
[36] G. Wheeler, Alkoxysilanes and the, consolidation of stone, Getty Publications, Los Angeles, USA, 2005.
[37] Rong Liu, et al., Preparation of three-component TEOS-based composites for stone conservation by sol–gel process, J Solgel Sci Technol 68 (2013) 19–30, doi:10.1007/s10971-013-3129-z.
[38] C. Salazar-Hernández, M.J.P. Alquiza, P. Salgado, J. Cervantes, TEOS–colloidal silica–PDMS-OH hybrid formulation used for stone consolidation, Appl Organomet Chem 24 (6) (2010) 481–488, doi:10.1002/aoc.1646.
[39] Y. Liu, J. Liu, Synthesis of TEOS/PDMS-OH/CTAB composite coating material as a new stone consolidant formulation, Construct Build Mat 122 (2016) 90–94, doi:10.1016/j.conbuildmat.2016.06.069.
[40] E.K. Kim, J. Won, J.Y. Do, S.D. Kim, Y.S. Kang, Effects of silica nanoparticle and GPTMS addition on TEOS-based stone consolidants, J Cult Herit 10 (2) (2009) 214–221, doi:10.1016/j.culher.2008.07.008.
[41] F.G. Adamopoulos, E.C. Vouvoudi, E. Pavlidou, D.S. Achilias, I. Karapanagiotis, TEOS-based superhydrophobic coating for the protection of stone-built cultural heritage, Coatings 11 (2) (2021) 135, doi:10.3390/coatings11020135.
[42] Giada MC Gemelli, et al., Alkoxysilane-based consolidation treatments: laboratory and 3-years In-Situ assessment tests on biocalcarenite stone from Roman Theatre (Cádiz), Construct Build Mat 312 (2021) 125398, doi:10.1016/j.conbuildmat.2021.125398.
[43] Jinghan Ding, et al., Quaternary ammonium silane modified Nanolime for the consolidation and antifungal of stone relics, Construct Build Mat 400 (2023) 132605, doi:10.1016/j.conbuildmat.2023.132605.
[44] E. Ksinopoulou, D. Dragatogiannis, A. Bakolas, et al., Physical and mechanical characteristics of TEOS-modified nanocomposites, J Polym Res 29 (2022) 196, doi:10.1007/s10965-022-03053-y.
[45] B. Sena da Fonseca, Current trends in stone consolidation research: an overview and discussion, Buildings 13 (2) (2023) 403, doi:10.3390/buildings13020403.
[46] S. Nguyen, D. Dobuzinsky, D. Harmon, R. Gleason, S. Fridmann, Reaction mechanisms of plasma-and thermal-assisted chemical vapor deposition of tetraethylorthosilicate oxide films, J Electrochem Soc 137 (7) (1990) 2209.
[47] L. Martinu, D. Poitras, Plasma deposition of optical films and coatings: a review, J Vac Sci Technol A 18 (6) (2000) 2619–2645, doi:10.1116/1.1314395.
[48] G. Tochitani, M. Shimozuma, H. Tagashira, Deposition of silicon oxide films from TEOS by low frequency plasma chemical vapor deposition, J Vac Sci Technol A 11 (2) (1993) 400–405, doi:10.1116/1.578743.
[49] H. Juárez, M. Pacio, T. Díaz, E. Rosendo, G. Garcia, A. García, G. Escalante, Low temperature deposition: properties of SiO2 films from TEOS and ozone by APCVD system, J Phys 167 (1) (2009) 012020.
[50] M. Abbasi-Firouzjah, S.I. Hosseini, M. Shariat, B. Shokri, The effect of TEOS plasma parameters on the silicon dioxide deposition mechanisms, J Non Cryst Solids 368 (2013) 86–92, doi:10.1016/j.jnoncrysol.2013.03.008.
[51] Sabrina Grassini, et al., Aesthetic coatings for silver based alloys with improved protection efficiency, Progr Organ Coat 72 (1–2) (2011) 131–137, doi:10.1016/j.porgcoat.2011.04.003.
[52] Sabrina Grassini, et al., Advanced plasma treatment for cleaning and protecting precious metal artefacts." Strategies for saving our cultural heritage, in: Proceedings of the international conference on conservation strategies for saving indoor metallic collections, Cairo, TEI of Athens, Athens, 2007, doi:10.1109/TIM.2010.2090191.
[53] Alessia Artesani, et al., Recent advances in protective coatings for cultural heritage–an overview, Coatings 10 (3) (2020) 217, doi:10.3390/coatings10030217.
[54] J.A. López-Barrea, O.G. Pimentel-Tinoco, R. Olayo-Valles, et al., Water permeability of quarry stone superficially modified by plasma polymerization of hexamethyldisiloxane at atmospheric pressure, J Coat Technol Res 11 (2014) 661–664, doi:10.1007/s11998-014-9585-8.
[55] Alho, Ana Patrícia RodriguesAs Gárgulas Do Mosteiro de Santa Maria Da Vitória: Função e Forma, Dissertação, Universidade de Lisboa, Lisboa, 2007.
[56] Y. Ding, A.T. Caldeira, C. Salvador, S. Grassini, E. Angelini, N. Schiavon, The inhibition of biodegradation on building limestone by plasma etching, ACTA IMEKO 10 (3) (2021) 209–217, doi:10.21014/acta_imeko.v10i3.1162.
[57] A. Tsakalof, P. Manoudis, I. Karapanagiotis, I. Chryssoulakis, C. Panayiotou, Assessment of synthetic polymeric coatings for the protection and preservation of stone monuments, J Cult Herit 8 (1) (2007) 69–72, doi:10.1016/j.culher.2006.06.007.
[58] C. Noè, C. Tonda-Turo, I. Carmagnola, M. Hakkarainen, M. Sangermano, UV-cured biodegradable methacrylated starch-based coatings, Coatings 11 (2) (2021) 127, doi:10.3390/coatings11020127.
[59] K.J. Stanienda-Pilecki, The importance of Fourier-transform infrared spectroscopy in the identification of carbonate phases differentiated in magnesium content, Spectroscopy 34 (6) (2019) 32–42.
[60] Dulce Esmeralda Ortega-Zavala, et al., An initial study on alkali activated limestone binders, Cem Conc Res 120 (2019) 267–278 http://doi.org/10.1016/j.cemconres.2019.04.002.
[61] V. Ramasamy, et al., FTIR-characterisation and thermal analysis of natural calcite and aragonite, Ind J Phys 77 (2003) 443–450.
[62] H.A. Budiarti, R.N. Puspitasari, A.M. Hatta, D.D. Risanti, Synthesis and characterization of TiO2@ SiO2 and SiO2@ TiO2 core-shell structure using Lapindo mud extract via sol-gel method, Procedia Eng 170 (2017) 65–71, doi:10.1016/j.proeng.2017.03.013.
[63] S.C. Deshmukh, E.S. Aydil, Investigation of SiO2 plasma enhanced chemical vapor deposition through tetraethoxysilane using attenuated total reflection Fourier transform infrared spectroscopy, J Vac Sci Technol A 13 (5) (1995) 2355–2367, doi:10.1116/1.579521.
[64] F. Hamelmann, U. Heinzmann, A. Szekeres, N. Kirov, T. Nikolova, Deposition of silicon oxide thin films in TEOS with addition of oxygen to the plasma ambient: IR spectra analysis, J Optoelectron Adv Mat 7 (1) (2005) 389–392.
[65] A. Bachar, et al., Composition and optical properties tunability of hydrogenated silicon carbonitride thin films deposited by reactive magnetron sputtering, Appl Surf Sci 444 (2018) 293–302.
[66] H. Yan, W. Yuanhao, Y. Hongxing, TEOS/silane-coupling agent composed double layers structure: a novel super-hydrophilic surface, Energ Procedia 75 (2015) 349–354, doi:10.1016/j.apenergy.2015.09.097.
[67] Ch Voulgaris, et al., RF power effect on TEOS/O2 PECVD of silicon oxide thin films, Surf Coat Technol 200 (1–4) (2005) 351–354.
[68] Cheng-Yang Wu, Wen-Cheng Chen, Day-Shan Liu, Surface modification layer deposition on flexible substrates by plasma-enhanced chemical vapor deposition using tetramethylsilane–oxygen gas mixture, J Phys D Appl Phys 41 (22) (2008) 225305, doi:10.1088/0022-3727/41/22/225305.
[69] M.H.H. Mahmoud, M.M. Rashad, I.A. Ibrahim, E.A Abdel-Aal, Crystal modification of calcium sulphate dihydrate in the presence of some surface-active agents, J Colloid Interface Sci 270 (1) (2004) 99–105, doi:10.1016/j.jcis.2003.09.023.
[70] M. Lettieri, M. Masieri, A. Morelli, M. Pipoli, M. Frigione, Oleo/hydrophobic coatings containing nano-particles for the protection of stone materials having different porosity, Coatings 8 (12) (2018) 429, doi:10.3390/coatings8120429.
[71] J. Huang, Y. Zheng, H. Li, Study of internal moisture condensation for the conservation of stone cultural heritage, J Cult Herit 56 (2022) 1–9, doi:10.1016/j.culher.2022.05.003.
[72] M.R. Talaghat, F. Esmaeilzadeh, D. Mowla, Sand production control by chemical consolidation, J Petrol Sci Engineer 67 (1–2) (2009) 34–40, doi:10.1016/j.petrol.2009.02.005.
[73] L. D'Arienzo, P. Scarfato, L. Incarnato, New polymeric nanocomposites for improving the protective and consolidating efficiency of tuff stone, J Cult Herit 9 (3) (2008) 253–260, doi:10.1016/j.culher.2008.03.002.
[74] Z. Jeckell, D. Patel, A. Herschberg, T. Choi, D. Barlaz, L. Bonova, D. Ruzic, Silicon dioxide deposited using atmospheric pressure plasma chemical vapor deposition for improved adhesion and water intrusion resistance for lightweight manufacturing, Surf Interf 23 (2021) 100989, doi:10.1016/j.surfin.2021.100989.